engineering proceedings

MDPI

Proceeding Paper

Research and Development of New High-Entropy Alloys for Hydrogen Storage †

Dagmara Varcholová [1,2,*], Lenka Oroszová [1], Katarína Kušnírová [1] and Karel Saksl [1,2]

1 Institute of Material Research, Slovak Academy of Sciences, Watsonova 47, 040 01 Košice, Slovakia; loroszova@saske.sk (L.O.)
2 Faculty of Materials, Metallurgy and Recycling, Technical University of Košice, Letná 9, 042 00 Košice, Slovakia
* Correspondence: dvarcholova@saske.sk; Tel.: +421-55-7922464

† Presented at the 30th International Conference on Modern Metallurgy—Iron and Steelmaking, Kosice, Slovakia, 27–29 September 2023.

Abstract: Hydrogen is a key element in the changing energy sector and presents an accessible alternative to conventional fossil fuel sources. In this work, a system of ten high-entropy alloys was prepared based on the Hume-Rothery rules. One of the biggest advantages of these alloys is their storage capacity, which reaches the highest value among all known alloys intended for hydrogen storage. Alloys based on Al-Ti-Nb-Zr elements with different atomic fractions show interesting accumulation capabilities with fast absorption kinetics and low specific gravity. Each alloy in this study underwent high-pressure gravimetric absorption and desorption tests. The main goals of this work were to prepare alloys with the lowest-possible specific gravity and the highest-possible storage capacity. One alloy from our system shows storage capacity values similar to commercial alloys, without any rare-earth elements.

Keywords: hydrogen; metal hydride; high-entropy alloys; storage capacity

check for updates

Citation: Varcholová, D.; Oroszová, L.; Kušnírová, K.; Saksl, K. Research and Development of New High-Entropy Alloys for Hydrogen Storage. *Eng. Proc.* **2024**, *64*, 9. https://doi.org/10.3390/engproc2024064009

Academic Editors: Branislav Buľko, Dana Baricová, Peter Demeter and Róbert Dzurňák

Published: 22 February 2024

1. Introduction

Hydrogen is currently the major topic worldwide because it can produce electricity very efficiently and without emissions. Therefore, it is ideal choice for powering vehicles such as cars and buses, as well as for various other modes of transportation, including shipping, aviation, and space transport. It has great potential for use as an alternative fuel, but only if it can be stored safely and efficiently. Agreements such as Clean Europe or Net Zero Emission by 2050 Scenario support actions to reduce CO_2 and increase carbon neutrality [1,2]. An "excellent" step forward in this direction is represented by the publication of M. Sahlberg et al. entitled "Superior hydrogen storage in high entropy alloys" [3]. In this study, the authors investigated the hydrogenation of a high-entropy alloy in a TiVZrNbHf solid solution with a BCC structure and found that it is possible to absorb an extremely large amount of hydrogen (2.7 wt.% hydrogen) this way. The amount of hydrogen corresponded to an H/M ratio of 2.5 and produced a world-record volumetric energy density of 219 kg H/m^3 [3]. High-entropy alloys are utilized for hydrogen storage due to their low specific weight, making them well-suited for applications in the automotive industry. High-entropy alloys are defined as a mixture of three to five elements with an atomic ratio ranging from 5 to 35%. Newer definitions also accept alloys with less than three main elements and an atomic ratio higher than 35%. It is evident from existing publications that high-entropy alloys can store a higher amount of hydrogen compared to known metal hydrides.

2. Materials and Methods

Alloys were prepared based on a predictive model by arc melting (Mini Arc Melting System MAM-1) from highly pure elements (>99.9 at.%) in a protective gas atmosphere

(Ar with purity 99.999%). Each sample was remelted five times to ensure homogeneity. Hardness analyses were performed on these alloy samples using a Wilson-Wolper Tukon 1102 Vickers indenter with a load of 0.3 $kgHV_{0.3}$. Subsequently, the samples underwent vibration grinding, resulting in a grain fraction below 45 µm. An EDX analysis was conducted on the prepared powder sample using a Tescan Vega-3LMU, Bruker Nano XFlash detector 410 m (Tescan, Brno, The Czech Republic) in secondary mode at an accelerating voltage of 20 kV. X-ray diffraction was performed using a Philips X Pert Pro (Malvern Panalytical, Almelo, The Netherlands), and the specific gravity was determined using the pycometric method (AccuPyc II 1345, (Micromeritics, Norcross, GA, USA)). The powder material, thus prepared and characterized, underwent high-pressure gravimetric analysis to assess its hydrogen absorption and desorption at the Institute of Nonclassical Chemistry, Leipzig. The sorption experiment consisted of four steps: The first step involved activation the sample by heating it to 350 °C for two hours in a vacuum. This was followed by the first cycle of absorption under conditions of 200 °C and a pressure 2×10^6 Pa of hydrogen. The next step was desorption at 370 °C in a vacuum. The final step involved a second absorption cycle under the same conditions as the first cycle

3. Results

Figure 1 shows a prediction map of the prepared alloys created based on Hume-Rothery's rules. The map is divided into two regions, namely the region of high-entropy phases and the region of amorphous phases. The alloys do not fit into the region of high-entropic phases but exhibit high-entropy properties. All of the produced alloys have a single-phase BCC structure.

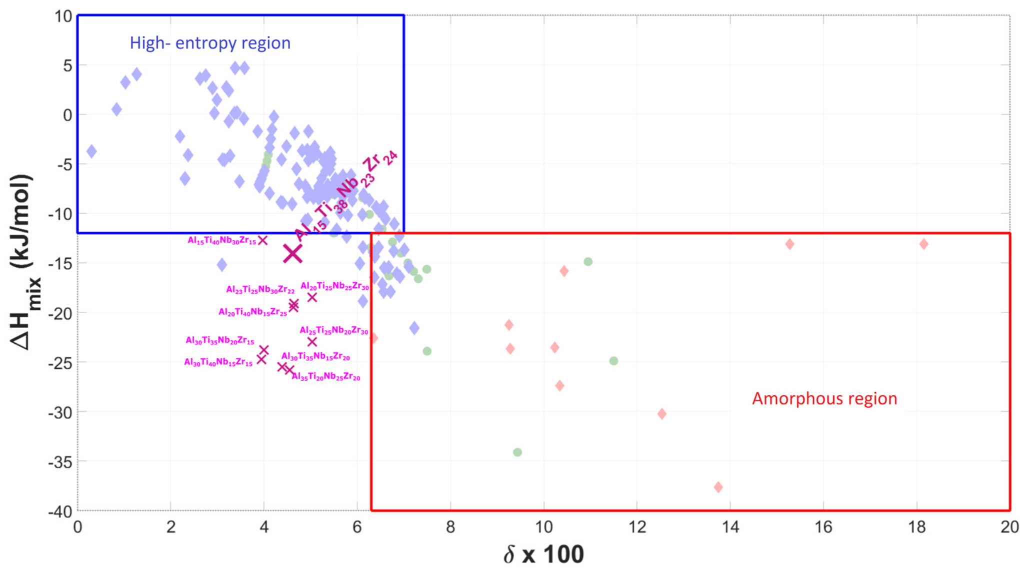

Figure 1. Prediction map of the prepared alloys.

Table 1 describes theoretical high-entropy properties that define the properties of the alloy and its storage capacity, where ΔH_{mix} a ΔS_{mix} are mixing enthalpy and enthropy, δr is a parameter of the difference in the size of the atomic diameters, and VEC is valence electron concentration [4,5], which were calculated in a program created by us in the Matlab programming language [6]. Table 2 describes the basic characteristics of the alloys, such as the results of the EDX analysis, microhardness, and specific gravity. One of the main goals of this work is to prepare a material with the lowest-possible specific gravity with regard to future applications. These alloys achieve significantly lower specific densities compared to commercial alloys such as $LaNi_5$ [7]. The alternative alloy names describe the precise atomic ratios after arc melting and EDX analysis.

Table 1. Overview table of the high-entropy properties of the prepared materials with different Al-Ti-Nb-Zr compositions.

Alloy	ΔH_{mix} [kJ/mol]	$\delta \times 100$	ΔS_{mix}	VEC
$Al_{30}Ti_{35}Nb_{15}Zr_{20}$	−25.50	4.39	11.10	3.85
$Al_{23}Ti_{25}Nb_{30}Zr_{22}$	−19.11	4.64	11.46	4.07
$Al_{30}Ti_{35}Nb_{20}Zr_{15}$	−23.80	3.99	11.10	3.90
$Al_{25}Ti_{25}Nb_{20}Zr_{30}$	−22.94	5.03	11.44	3.95
$Al_{15}Ti_{38}Nb_{23}Zr_{24}$	−14.08	4.61	11.08	4.08
$Al_{35}Ti_{20}Nb_{25}Zr_{20}$	−25.82	4.54	11.29	3.90
$Al_{30}Ti_{40}Nb_{15}Zr_{15}$	−24.72	3.95	10.78	3.85
$Al_{20}Ti_{25}Nb_{25}Zr_{30}$	−18.46	5.04	11.44	4.05
$Al_{20}Ti_{40}Nb_{15}Zr_{25}$	−19.48	4.62	10.97	3.95
$Al_{15}Ti_{40}Nb_{30}Zr_{15}$	−12.72	3.96	10.78	4.15

Table 2. Overview table of the material properties of the prepared materials with different Al-Ti-Nb-Zr compositions.

Alloy	EDX	Microhardness [$HV_{0.3}$]	Density [$g.cm^{-3}$]
$Al_{30}Ti_{35}Nb_{15}Zr_{20}$	$Al_{30}Ti_{34}Nb_{14}Zr_{22}$	532 ± 93.41	5.311 ± 0.009
$Al_{23}Ti_{25}Nb_{30}Zr_{22}$	$Al_{23}Ti_{27}Nb_{28}Zr_{22}$	453 ± 43.79	6.011 ± 0.006
$Al_{30}Ti_{35}Nb_{20}Zr_{15}$	$Al_{31}Ti_{36}Nb_{20}Zr_{13}$	542 ± 20.81	5.52 ± 0.14
$Al_{25}Ti_{25}Nb_{20}Zr_{30}$	$Al_{24}Ti_{26}Nb_{21}Zr_{30}$	444 ± 7.04	5.83 ± 0.02
$Al_{15}Ti_{38}Nb_{23}Zr_{24}$	$Al_{16}Ti_{38}Nb_{23}Zr_{23}$	376 ± 9.039	5.87 ± 0.012
$Al_{35}Ti_{20}Nb_{25}Zr_{20}$	$Al_{33}Ti_{23}Nb_{24}$ Zr_{20}	747 ± 31.15	5.811 ± 0.008
$Al_{30}Ti_{40}Nb_{15}Zr_{15}$	$Al_{28}Ti_{38}Nb_{16}Zr_{18}$	587 ± 18.5	5.461 ± 0.017
$Al_{20}Ti_{25}Nb_{25}Zr_{30}$	$Al_{21}Ti_{26}Nb_{26}Zr_{27}$	470 ± 141.3	6.151 ± 0.019
$Al_{20}Ti_{40}Nb_{15}Zr_{25}$	$Al_{19}Ti_{41}Nb_{15}Zr_{25}$	353 ± 10.6	5.641 ± 0.004
$Al_{15}Ti_{40}Nb_{30}Zr_{15}$	$Al_{14}Ti_{39}Nb_{29}$ Zr_{18}	398 ± 20.9	6.11 ± 0.02

The measurement scheme using high-pressure thermogravimetric analysis is shown in Figure 2. The results of the high-pressure analysis of hydrogen absorption and desorption on the $Al_{15}Ti_{38}Nb_{23}Zr_{24}$ alloy are divided into four graphs, which are shown in Figure 3. The first deals with the change in corrected weight and temperature during individual measurement steps. The following graph describes the actual absorption or desorption of hydrogen during the measurement of how many milligrams of hydrogen were stored in one gram of the sample. The third graph describes the change in the hydrogen-to-metal atom ratio (H/M ratio). The last graph shows the absorption kinetics. The yellow area shows unbalanced conditions, such as a change in pressure or temperature.

Table 3 describes the values of absorbed, residual, and desorbed hydrogen, with the last column indicating the efficiency of the cycle. The highest storage capacity was achieved by the $Al_{15}Ti_{38}Nb_{23}Zr_{24}$ sample, with a value of 1.61 wt.% and an H/M ratio of 1.05.

Table 3. Sorption properties of the alloys.

Alloy	Absorption H [wt.%/H/M]	Residual H [wt.%/H/M]	Desorption H [wt.%/H/M]	Cycle Efficiency [%]
$Al_{30}Ti_{35}Nb_{15}Zr_{20}$	1.28/0.74	0.46/0.26	0.82/0.48	64.86
$Al_{23}Ti_{25}Nb_{30}Zr_{22}$	1.06/0.69	0.25/0.16	0.81/0.53	76.81
$Al_{30}Ti_{35}Nb_{20}Zr_{15}$	0.98/0.54	0.27/0.15	0.71/0.39	72.22
$Al_{25}Ti_{25}Nb_{20}Zr_{30}$	1.23/0.82	0.41/0.27	0.82/0.55	67.07
$Al_{15}Ti_{38}Nb_{23}Zr_{24}$	1.61/1.05	0.62/0.40	0.99/0.65	61.90
$Al_{35}Ti_{20}Nb_{25}Zr_{20}$	0.79/0.48	0.18/0.10	0.61/0.38	79.16
$Al_{30}Ti_{40}Nb_{15}Zr_{15}$	1.10/0.63	0.37/0.22	0.73/0.41	65.08
$Al_{20}Ti_{25}Nb_{25}Zr_{30}$	1.28/0.86	0.43/0.29	0.85/0.57	66.28
$Al_{20}Ti_{40}Nb_{15}Zr_{25}$	1.28/0.79	0.54/0.33	0.74/0.46	58.23
$Al_{15}Ti_{40}Nb_{30}Zr_{15}$	1.33/0.88	0.30/0.20	1.03/0.68	77.27

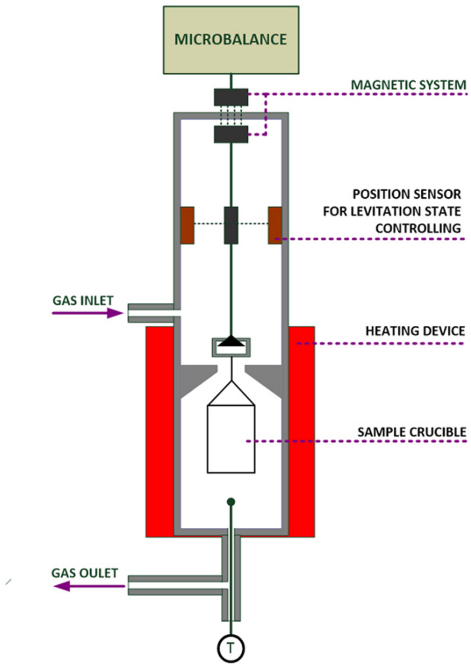

Figure 2. Scheme of the high-pressure thermogravimetric analysis [8].

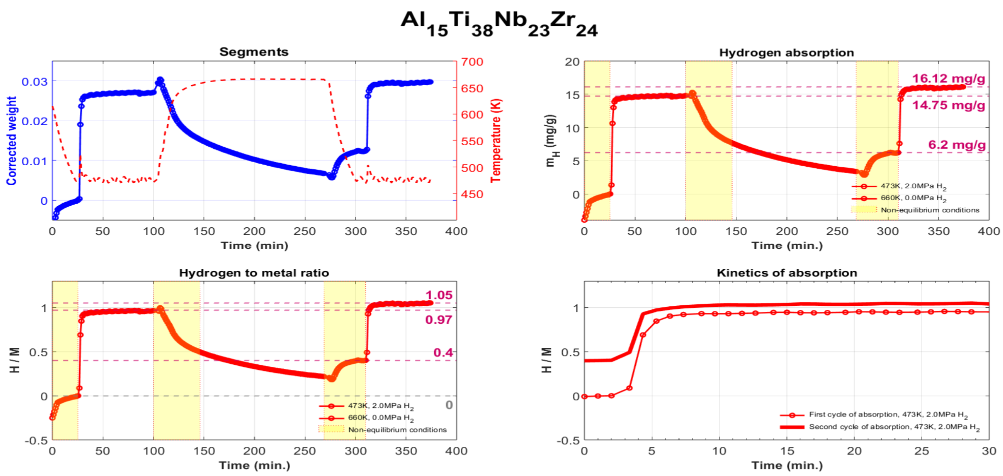

Figure 3. Progress of the high-pressure analysis of hydrogen absorption and desorption for the $Al_{15}Ti_{38}Nb_{23}Zr_{24}$ alloy.

4. Conclusions

Based on the prediction theory compiled according to the Hume-Rothery rules, the emergence of high-entropy phases was assumed. Most of the alloys show the one BCC phase, which was partially confirmed via X-ray diffraction. Samples with the elemental composition Al-Ti-Nb-Zr align with our goal of reducing specific weight, with the highest specific weight being recorded for the $Al_{20}Ti_{25}Nb_{25}Zr_{30}$ sample at 6.15 g.cm^{-3}. All samples underwent high-pressure gravimetric analysis for hydrogen absorption and desorption in two cycles at 200 °C and a hydrogen pressure of 2.10^{6} Pa. No rare-earth elements were used in the production of the samples, which also reduced the cost of manufacturing the alloys. The $Al_{15}Ti_{38}Nb_{23}Zr_{24}$ alloy reached a storage capacity of 1.61 wt.% and a density of 5.87 g.cm^{-3}, comparable to the commercial material $LaNi_5$, which reaches a storage capacity value of 1.4 wt.% and a density of 7.95 g.cm^{-3} [7].

Author Contributions: Conceptualization, D.V.; validation, D.V. and K.S.; formal analysis, D.V. and L.O.; investigation, D.V., K.S., K.K. and L.O.; resources, D.V., L.O. and K.K.; data curation, D.V. and K.S.; writing—original draft preparation, D.V.; writing—review and editing, D.V., K.S., K.K. and L.O.; visualization, D.V.; supervision, D.V., K.S. and L.O.; project administration, D.V., K.K. and L.O.; funding acquisition, D.V. and K.S. All authors have read and agreed to the published version of the manuscript.

Funding: This work was supported by the Slovak Research and Development Agency under the contract no. APVV-20-0205, APVV-21-0274. The authors are grateful to the Scientific Grant Agency of the Ministry of Education, Science, Research and Sport of the Slovak Republic and the Slovak Academy of Sciences VEGA, project no. 2/0039/22, and the international project EIG CONCERT-Japan/2021/215/EHSAL.

Institutional Review Board Statement: Not applicable.

Informed Consent Statement: Not applicable.

Data Availability Statement: Data will be made available upon request.

Conflicts of Interest: The authors declare no conflicts of interest. The funders had no role in the design of this study; in the collection, analyses, or interpretation of data; in the writing of the manuscript; or in the decision to publish the results.

References

1. Annual Activity Report 2020. 2020. Available online: https://www.clean-hydrogen.europa.eu/system/files/2021-06/FCH-20-001-Annual%2520report%25202020%2520%2528ID%252011531857%2529.pdf (accessed on 8 February 2024).
2. IEA. *World Energy Model*; IEA: Paris, France, 2021. Available online: https://www.iea.org/reports/world-energy-model (accessed on 8 February 2024).
3. Züttel, A. Materials for hydrogen storage. *Mater. Today* **2003**, *6*, 24–33. [CrossRef]
4. Murty, B.S.; Yeh, J.W.; Ranganathan, S.; Bhattacharjee, P.P. *High-Entropy Alloys*, 1st ed.; Elsevier: Amsterdam, The Netherlands, 2014.
5. Guo, S.; Liu, C.T. Phase stability in high entropy alloys: Formation of solid-solution phase or amorphous phase. *Prog. Nat. Sci. Mater. Int.* **2011**, *21*, 433–446. [CrossRef]
6. MATLAB—MathWorks. IsoSORP. Available online: https://www.mathworks.com/products/matlab.html (accessed on 21 April 2023).
7. Joubert, J.M.; Paul-Boncour, V.; Cuevas, F.; Zhang, J.; Latroche, M. LaNi5 related AB5 compounds: Structure, properties and applications. *J. Alloys Compd.* **2021**, *862*, 158163. [CrossRef]
8. Joubert, J.M.; Paul-Boncour, V.; Cuevas, F.J. Sorption Analysis under Extreme Conditions—TA Instruments. Available online: https://www.tainstruments.com/isosorp/ (accessed on 21 April 2023).